NACA TN 3214

NATIONAL ADVISORY COMMITTEE FOR AERONAUTICS

TECHNICAL NOTE 3214

FUNDAMENTAL STUDY OF EROSION CAUSED BY STEEP PRESSURE WAVES

By B. G. Rightmire and J. M. Bonneville

Massachusetts Institute of Technology

Washington
June 1954

NATIONAL ADVISORY COMMITTEE FOR AERONAUTICS

TECHNICAL NOTE 3214

FUNDAMENTAL STUDY OF EROSION CAUSED BY STEEP PRESSURE WAVES

By B. G. Rightmire and J. M. Bonneville

SUMMARY

A fundamental study of erosion caused by steep pressure waves has been carried out. It is believed that the study gives an insight to the possible causes of damage in high-speed sleeve bearings. In particular, the effect on annealed copper surfaces of steep-fronted pressure waves in oil has been studied, the general conclusion being that cavitation of the oil is the probable cause of damage.

INTRODUCTION

It is a matter of experience that a high-speed sleeve bearing subject to a fluctuating load may develop damage similar in appearance to that produced by hydraulic cavitation (ref. 1). Such damage has been observed, for example, in the bushings of a spur-geared supercharger drive for an aircraft before the gear teeth have been run-in. With properly run-in gears it has been found that no damage is produced (ref. 2).

The present investigation deals with one aspect of the problem of explaining how this damage occurs. Since the two conditions of high speed and fluctuating load both appear to be necessary, a reasonable explanation would be that cavitation in the oil film is the cause. Alternatively, the fluctuating load might be high enough to transmit stresses through the oil film capable of damaging the bearing material. It is known that metals can be plastically deformed by suddenly applied loads transmitted through thin films of liquid (ref. 3).

At the time the present project was undertaken still a third possibility existed as the result of work done by Ackeret and De Haller (refs. 4 to 6). These authors have studied the effect produced on metal and glass surfaces by impingement of pressure waves in liquid. They found that a few hundred thousand impingements of "steep-fronted" waves sufficed to damage their specimens. The peak pressures reached during these experiments were reported to be less than the static yield stress of the test materials. On the other hand, a pressure wave varying sinusoidally with time and having a somewhat higher peak value than the steep-fronted wave produced no effect, even after nearly a million applications. Ackeret and De Haller concluded that a steep-fronted pressure wave in

liquid could produce damage similar to that caused by cavitation, even though the normal stress was uniformly applied over the test surface and the peak normal stress was less than that required to cause yielding under static conditions.

In view of the possible application to damage in bushings, it was decided to build a "liquid-impact" apparatus somewhat like that of Ackeret and De Haller but with provision for measuring the steepness and amplitude of the pressure waves. This apparatus was to be used to try to check the results of Ackeret and De Haller and to investigate the effects of amplitude and steepness of the pressure waves.

This investigation was conducted at the Massachusetts Institute of Technology under the sponsorship and with the financial assistance of the National Advisory Committee for Aeronautics.

APPARATUS

A diagrammatic sketch of the apparatus is given in figure 1. The ram of an electric or air hammer was arranged to strike a hardened steel piston lapped into a bronze bushing (not shown) pressed into a steel tube that formed the body of the apparatus. The outer diameter of this tube was $1\frac{3}{16}$ inches. The test chamber, filled with oil under controlled static pressure, was closed at one end by the lapped-in piston and at the other by a Duralumin rod sealed by an annular Neoprene washer and screw cap (not shown) at the end of the steel tube. A disk-shaped copper specimen could be attached to the face of the Duralumin rod. The piston, test chamber, and Duralumin rod were all 3/4 inch in diameter, there being no offset nor obstruction to interfere with the wave motion in the oil.

In order to determine the normal stress at the face of the Duralumin rod, the axial strain in the rod was measured as a function of time by means of a wire resistance strain gage connected to a cathode-ray oscilloscope. Since the elastic properties of the rod and the factor of the gage were known, the oscillogram was readily interpreted to give the stress wave transmitted along the Duralumin rod from the oil (or specimen, if present). At a given point on the rod, the stress due to this transmitted wave was essentially the same function of time as that at the interface between rod and oil (or rod and specimen, if present), since damping of the wave in Duralumin was found to be small. (This point was checked by a comparison of the oscillograms from two gages spaced about 4 feet apart along the rod.)

The blows of the hammer were repeated at essentially a uniform rate, so that it was possible to adjust the internal sweep of the oscilloscope

to give a steady trace on the screen. The interval between hammer blows (about 1/60 second) was so great compared with the rise time of the stress wave, however, that no information about the rate of stress rise could be gleaned until an external sweep circuit was constructed for which the writing speed and repetition rate were independently adjustable. The gage nearer the test chamber triggered this sweep circuit; the desired signal was taken from the second gage (fig. 1). To simplify the construction, this sweep was exponential instead of linear.

A delay circuit was incorporated in the output from the trigger gage so that not only the head end of the wave but any selected portion could be viewed on the oscilloscope.

The lead rod shown in figure 1 absorbed an appreciable fraction of the energy of the wave propagated along the gage rod, thereby reducing the reflections coming back to the specimen from the downstream (right-hand) end of the equipment.

In the photograph of figure 2 the air hammer is at the right; attached to it is the steel test chamber from which protrudes horizontally the Duralumin rod on which the strain gages are mounted. The tank for the nitrogen pressurizing the test oil is in the center of the picture, while the pressure gage and oil tank are in the left foreground. The valve at the bottom of the oil tank and those on the test chamber were provided so that air could be readily bled from the latter. The Duralumin rod was retained in position against the force of the oil in the test chamber by means of the lightweight arrangement of piano wire and rubber springs shown in figure 2.

A general view of the whole equipment is given in figure 3. The coil of lead rod is seen in the foreground.

A modified form of the apparatus is shown diagrammatically in figure 4. In order to reduce the effect of reflections from the upstream end of the piston, the original $3\frac{1}{4}$- inch one was replaced by a 9-foot piston rod.

The method of attaching a specimen to the Duralumin gage rod is shown in figure 5(a). This method was also used initially when the Duralumin gage rod had been replaced by steel. In order to ensure a one-dimensional stressing of the specimen and also to eliminate the hole in its center, the method of attachment shown in figure 5(b) was adopted. This had the disadvantage of distorting somewhat the wave transmitted to the gage rod. A specimen shaped to experience a hydrostatic stress is shown mounted in figure 5(c).

Auxiliary equipment used in this investigation consisted of a small tubular electric furnace for annealing the copper specimens in an atmosphere of purified helium, an X-ray diffraction apparatus for detecting cold-work in the specimens, electropolishing and etching equipment, a Tukon (Knoop) hardness tester, and various tensile and compressive testing machines.

PROCEDURE

The specimens were all made from the same bar of annealed, oxygen-free, high-conductivity copper. Twenty specimen disks 5/8 inch in diameter and 1/8 inch thick, polished on 3-0 emery paper, were annealed simultaneously in an atmosphere of helium purified by passage through a tube of activated charcoal immersed in a bath of liquid nitrogen. The temperature was automatically controlled at 500° C; the annealing time was 1 hour. The specimens were allowed to cool in the furnace.

Every specimen was photographed in the X-ray diffraction apparatus and rejected unless it showed the pattern of sharply defined spots characteristic of annealed material (see fig. 6). Some specimens were then electrolytically polished to a mirror finish.

The liquid medium was a refined white mineral oil known as "Clearteck." Its viscosity was about ten times that of water at room temperature.

All tests were run at room temperature; the static pressure was controllable over the range from atmospheric to 500 lb/sq in. gage. The time of test varied between 5 minutes and 2 hours. The repetition rate for the electric hammer was 25 to 30 blows per second in all tests, while that of the air hammer was 40 to 50 blows per second.

The figure on the oscilloscope screen was manually traced on graph paper, rather than being photographed, since speed and simplicity were needed, rather than great accuracy. The graph paper was placed on the table supporting the oscilloscope, together with an Oscillotracer, an instrument consisting essentially of a piece of glass tilted at 45° to the horizontal. By suitably arranging the paper and Oscillotracer in front of the oscilloscope and looking vertically downward through the glass, one could see a bright image of the figure superposed on the graph paper. This image was then drawn on the paper. (See fig. 7.) The procedure used in analyzing the oscillograms is given in the appendix.

RESULTS AND DISCUSSION

For the first experiments, low static pressures were used (100 to 120 lb/sq in. gage), as were used by Ackeret and De Haller. It was found that cold-work detectable by X-ray diffraction could be obtained after a 15-minute exposure to a pressure wave producing a compressive stress amplitude of 940 lb/sq in. and a rate of rise of 150 lb/sq in./μsec. The results were comparable with those shown in figure 6.

In order to test the effect of changing the rate of pressure rise while the maximum pressure was held fixed, a special piston was made which was turned down to $\frac{1}{4}$-inch diameter for a $1\frac{1}{16}$-inch length at the end struck by the ram of the hammer. This small-diameter "tail" acted like a compression spring inserted between the ram and piston and reduced the rate of pressure rise to 30 lb/sq in./μsec without change in the peak pressure. The cold-work obtained under these conditions appeared to be the same as that for the wave of 150 lb/sq in./μsec when corresponding X-ray photographs were compared.

An increase in static pressure was then found to reduce the amount of cold-work as estimated by the X-ray technique. To check this, a series of tests was performed, in which all specimens were run under conditions identical except for the value of static pressure. At least two specimens were run under each condition. The results, which are given in table 1, comprise microhardness and weight-loss measurements. These results were corroborated qualitatively by X-ray photographs.

Microhardness determinations were made at eight points on the surface of each specimen; the average of these is listed in the table. These results are plotted in figure 8, which shows that both the weight loss and the increment in Knoop hardness decrease as the static pressure increases. This tendency is to be expected if cavitation is the cause since a sufficiently high pressure inhibits the formation of cavitation bubbles. On the other hand, it is difficult to see how the direct action of the pressure waves could bring about such a result.

A visual check on the occurrence of cavitation in the apparatus was attempted by installing glass windows in the tube wall so that the specimen surface and adjacent liquid could be illuminated and observed. Momentary "flashes," presumably of vapor, were observed whose appearance coincided with slight irregularities in the operation of the electric hammer. Furthermore, even though all visible air bubbles were removed before starting the machine, it was sometimes found that a few bubbles could be seen after the machine was stopped.

Since all damage and cold-work observed up to this point were almost certainly due to cavitation, it was decided to replace the electric hammer with a pneumatic one of greater power. It was hoped thereby to produce waves of sufficient amplitude and steepness to cause damage in the absence of cavitation.

When the air hammer was first installed, a test chamber 29 feet long was tried out, with the thought that the wave front might steepen noticeably as the wave progressed toward the specimen, the amplitude remaining constant. This scheme failed, both amplitude and steepness being less than that attained with a shorter column of oil. The reason for this failure was not determined, but it is believed that macroscopic air bubbles may have been present, the large volume of the system leading to uncertainties in this respect. Viscous damping may also have contributed to this failure, since a decrease in amplitude would tend to reduce the steepness.

Eventually the opposite extreme was tried, namely, a very short oil column approximately 0.1 inch in length, so that many reflections of the original wave were practically superposed on one another. With this arrangement, pressure amplitudes as high as 3,300 lb/sq in. and rates of pressure rise up to 270 lb/sq in./μsec were attained. (See fig. 7(d).) The oscillograms showed, however, a very serious tensile peak under these extreme conditions, and even under milder ones the ratio of peak tension to peak compression (T/C ratio) was approximately 1:4. (See figs. 7(b) and 7(c).). These tensile peaks were accounted for as the result of reflections from the upstream end of the $3\frac{1}{4}$-inch piston. Since the use of a static pressure greater than 500 lb/sq in. gage was impracticable, the liquid was required to transmit very considerable tensions for brief periods, and the occurrence of cavitation was highly probable.

Cold-work and damage were obtained with this new arrangement, but the uncertainty with regard to the cause persisted. The presence of cavitation in those tests resulting in the most cold-work and damage was suggested not only by the tensile peaks of the oscillograms but also by foaming of the oil leaking past the specimen and Neoprene sealing ring on the gage rod and also by a peculiar "burnt" odor of the leakage. The burnt odor was presumably due to oxidation, the oxygen being released by cavitation (ref. 7).

The depth to which the cold-work extended beneath the surface was determined for several specimens by electrolytically etching away successive thin layers, an X-ray diffraction picture of the exposed surface being made after each layer was removed. (See fig. 9.) The maximum penetration of cold-work found was 0.11 centimeter and on most specimens the depth did not exceed about 0.01 centimeter. These observations are readily explained as an effect of cavitation because it would give rise

to localized high pressures that would create small regions of high shear stress close to the surface of the specimen. The regions would not, however, penetrate far beneath the surface. By contrast, the distance from the extreme front of the applied pressure wave to the peak was about 2 inches as it traversed the metal. The 1/8-inch-thick specimen was thus subjected to a nearly uniform normal stress at any given instant. Cold-work due to this cause would, therefore, be expected to be uniform throughout the thickness of the specimen.

Since it is known that application of a hydrostatic pressure does not cause appreciable plastic deformation (ref. 8), precautions were taken to ensure a one-dimensional application of normal stress to the specimens (fig. 5(b)). The results on specimens shielded in this way did not differ in regard to depth of cold-work (or in any other observable respect) from those obtained on imperfectly shielded specimens (fig. 5(a)) subject to at least some hydrostatic stressing by the pressure wave. To obviate any possible doubt as to the effect of clearance around the rim, several specimens were tested that had been especially machined to a diameter of about 1/2 inch. There was thus a 1/8-inch clearance all around the specimen (fig. 5(c)). The behavior of these specimens was again the same as that of the other two types. The cold-work penetrated to depths of only a few hundredths of a centimeter in all cases.

All the above evidence points to the conclusion that the cold-work observed up to this point of the investigation was the result of cavitation.

The final phase of the work was devoted to detecting the effect of the pressure waves themselves on the test specimens. As the first step in this program, it was decided to try to reduce the likelihood of cavitation by cutting down the peak tension occurring for a given magnitude of peak compression. That is, the ratio of peak tension to peak compression (T/C ratio) was to be decreased. An analysis of the wave propagation in the apparatus showed that this ratio could probably be made smaller if a long rod were substituted for the $3\frac{1}{4}$-inch piston (fig. 4).

Accordingly, a 9-foot-long piston rod was installed, with the result that the T/C ratio was cut approximately in half, from about 1:4 to about 1:8 (figs. 7(e) and 7(f)). Peak pressures of 5,500 lb/sq in. and rates of pressure rise of 350 lb/sq in./μsec were obtained. (The maximum time of test was 2 hours or approximately 320,000 applications.) This low value of the T/C ratio was found, however, only with a plain gage rod. When a specimen was attached to the gage rod the T/C ratio apparently increased, as a result of the presence of the fastening arrangement. Several tests were made, nevertheless, on 1/8-inch-thick

copper specimens, each specimen being run for 10 minutes under a peak pressure of 4,500 lb/sq in. (fig. 7(g)). No burnt smell of the oil was present during these tests. Some slight cold-working was suggested by X-ray diffraction pictures of both the upstream and downstream faces of the specimens, but the results were inconclusive.

In order to eliminate the uncertainties associated with fastening the specimens to the gage rod, it was decided to use a copper bar as gage rod and specimen combined. Oxygen-free high-conductivity copper was not available, so that an 8-foot bar of cold-drawn commercial copper (tough pitch) was employed. A 12-inch length at the upstream end of this bar was annealed in an atmosphere of helium. X-ray diffraction photographs at the upstream end and at several points along the length of the annealed portion had the appearance of figure 9(a). In order to measure the permanent strain that might occur under test in the annealed length, four strain gages were installed spaced 1 inch apart, the first gage being 5 inches from the upstream end of the copper bar. Other strain gages were cemented to the unannealed portion for determining in the usual way the shape and amplitude of the wave passing along the bar.

Before making a test on this long specimen it was desired to establish the static stress-strain curve of the annealed copper for comparison with the results of the liquid impact. For this purpose, several standard 0.505-inch-diameter tensile specimens were machined from a piece of the bar used as the specimen. One of these was tested unannealed and found to have a Young's modulus of 16.7×10^6 lb/sq in. and an elastic limit of 45,000 lb/sq in. Two other tensile specimens were annealed in the helium furnace, checked by X-ray diffraction, and tested. The resulting stress-strain curve is shown in figure 10.

The copper specimen bar was then subjected to a series of 5-minute tests in the liquid-impact apparatus under the action of waves of several intensities, the wave of lowest intensity being applied first. The peak pressure of the wave transmitted along the bar and the permanent strains recorded by the wire gages at the conclusion of every test are given in table 2. The oscillogram for the wave of highest intensity is shown in figure 7(h).

The results from tests 4 and 5 of table 2 are plotted in figure 11. The strains at the head end of the specimen bar, estimated by extrapolation in figure 11, together with the corresponding peak compressive stress from table 2, are plotted in figure 10 for comparison with the static results. It will be observed that the dynamic test points lie considerably above the static curve, in qualitative agreement with the results of Kolsky (ref. 9).

The question arises as to why the permanent strains shown in table 2 decreased with distance from the upstream end of the bar. It would be expected that the strain would decrease with distance after the passage of only a few stress waves but that the elastic limit of a greater and greater length would be raised to the amplitude of the applied stress as more and more waves traversed the bar. Eventually, a uniform permanent strain would be expected to exist throughout the part that initially had been uniformly annealed.

Actually, the annealing method used tended to produce a variable anneal since a 7-foot length of the bar projected from the furnace into the atmosphere, thus acting as a cooling fin. An estimate of the temperature distribution along the bar has been made based on an analysis by Rizika and Rohsenow (ref. 10). The computed values, plotted in figure 12, show that, although the indicated temperature of the furnace was 500° C, the temperature of the bar varied from approximately 465° C at the end to 425° C at a point 8 inches from the end. At sections of of the bar subjected to the lower annealing temperatures the cold-work remaining in the bar was thus greater and less permanent strain was required to raise the elastic limit of the annealed sections to a given value.

The fact that the X-ray diffraction pictures of the bar showed sharply defined spots does not prove a uniform anneal. In this connection some static compressive tests performed on annealed commercial copper specimens are important, since they indicate that a compressive stress of 6,000 lb/sq in. was needed to influence the X-ray diffraction pattern. This stress was well beyond the yield point, as may be seen from figure 10.

CONCLUSIONS

The following general conclusions were drawn from the present investigation of causes of damages in high-speed sleeve bearings:

1. All cold-work and damage observed on the disk-shaped copper specimens were due to cavitation caused by the momentary tensile stresses produced in the fluid by the action of the hammer.

2. The most intense waves used in this investigation, having an amplitude of about 5,500 lb/sq in. and an initial rate of rise of about 350 lb/sq in./μsec, were incapable of producing cold-work detectable by the X-ray-diffraction method or of causing any damage to the copper specimens within the maximum time of test (2 hours, corresponding to approximately 320,000 applications).

3. The effect of the suddenly applied waves in producing permanent strain was less than that of a statically applied stress of equal magnitude.

4. Cavitation is the probable cause of damage in high-speed sleeve bearings.

Massachusetts Institute of Technology,
Cambridge, Mass., April 16, 1953.

APPENDIX A

ANALYSIS OF OSCILLOGRAMS

The oscillogram of figure 7(a) was obtained with the apparatus arranged as in figure 1, except that a steel gage rod without specimen was used. The scale for the pressure was determined by means of an over-all calibration of the strain-gage and amplifier circuits, accomplished by shunting the unloaded strain gage with a known resistance. The resulting known change in resistance of the gage circuit caused a definite deflection of the oscilloscope trace, which by computation was related to a definite applied stress. For details, see reference 11.

The full and dotted curves of figure 7(a) were obtained from different strain gages spaced 4.1 inches apart along the steel gage rod, the gage giving the full curve being closer to the test chamber than the other.

The sweep being exponential, the relation between distance x and time t is

$$(x_o - x)/x_o = \exp(-t/RC) \tag{1}$$

where x_o is the total extent of the curve along the x-axis. Whence it follows that the time constant

$$RC = (t_2 - t_1)/\log_e\left[(x_o - x_1)/(x_o - x_2)\right] \tag{2}$$

where subscripts 1 and 2 refer to any two points along the x-axis. The time interval $t_2 - t_1$ corresponding to points 1 and 2 marked in figure 7(a) is that required for the strain wave in the steel gage rod to traverse the 4.1-inch distance between the two gages mentioned above, so $t_2 - t_1$ = Distance/sound velocity in steel = 4.1 in./0.2 in/μsec = 20.5 μsec. Substitution of distances measured on the figure thus yields

$$RC = 190 \text{ μsec} \tag{3}$$

The rate of pressure (compressive stress) rise dp/dt at the head end of the wave is computed with the aid of equation (1):

$$\frac{dp}{dt} = \frac{dp}{dx}\frac{dx}{dt} = \frac{dp}{dx}\frac{x_o - x}{RC} \tag{4}$$

Estimating the average value of dp/dx near point 1 as $(p_a - p_1)/(x_a - x_1)$, one obtains

$$\left(\frac{dp}{dt}\right)_1 = \frac{p_a - p_1}{x_a - x_1}\frac{x_o - x_1}{RC} = \frac{1{,}380 \text{ lb/sq in.}}{0.16 \text{ in.}} \times \frac{2.68 \text{ in.}}{190 \text{ μsec}} = 122 \text{ lb/sq in./μsec} \tag{5}$$

The 10 small peaks following the first at point a in figure 7(a), such as b and c, are caused by reflections from the upstream end of the 3.25-inch piston, as can be seen by computing, for example, the time interval $t_b - t_a$. From equation (2), $t_b - t_a$ is found to be 32.0 μsec, while the time required for a wave to traverse twice the piston length is $2 \times 3.25/0.2 = 32.5$ μsec. These two values agree within the limits of experimental error.

The high peaks at d and f are the result of reflections through the oil column from the piston head, as can be checked by noting that $t_d - t_a = 328$ μsec from equation (2). The speed of sound in the oil can thus be estimated as $2 \times 9.75/328 = 0.0595$ in./μsec = 4,950 ft/sec, a reasonable value.

The tensile peak at g marks a reflection from the downstream end of the gage rod that, owing to the law of transmission at a steel-oil interface, gives rise to a tension in the liquid of about 7 percent of the magnitude of the peak itself.[1]

---

[1]Ratio of transmitted pressure to incident pressure is

$$\frac{2}{1 + \frac{\rho_S c_S}{\rho_O c_O}} = \frac{2}{1 + \frac{3.90}{0.135}} \approx 0.07$$

where ρ is density, c is velocity of sound, S is steel, and O is oil.

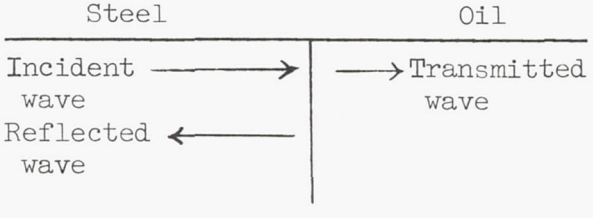

The tensile peak at e is, therefore, the highest tension occurring in the oil at the steel surface. The ratio T/C of peak tension to peak pressure is thus about 1:4.

In an effort to increase the peak pressure and rate of pressure rise, the oil chamber was progressively shortened, with the results shown in figures 7(b) to 7(d). The high values of these quantities noted in figure 7(d) were accompanied by a rise in peak tension that was disastrous as far as prevention of cavitation was concerned. These high tensile peaks were due principally to reflections from the upstream end of the piston but were aggravated by the specimen-holding device (fig. 5(b)), which was present when these last three oscillograms were made.

To reduce the T/C ratio as far as possible and still retain high values of peak pressure and rate of pressure rise, a 9-foot piston rod was installed, as shown diagrammatically in figure 4. Figures 7(e) and 7(f) show the marked improvement obtained with this piston rod in conjunction with a plain gage rod without specimen. The large tensile peak is again due to reflection from the downstream end of the gage rod and, therefore, produces a tension in the liquid only 7 percent of its own amplitude. The T/C ratio is seen to be less than 1:8. In figure 7(e) the tensile peaks b, d, and f are reflections from the downstream end of the gage rod, which was approximately 9 feet from the gage. The compressive peaks c, e, and g are reflections from the upstream end of the piston rod, which was approximately 9 feet long. The two types of reflected wave passed the gage almost simultaneously, traveling in opposite directions.

Unfortunately, this favorable value of the T/C ratio was not found when a specimen was attached to the gage rod as in figure 5(b)). An oscillogram obtained with the specimen and holder in place is shown in figure 7(g).

The oscillogram obtained during the final run on the copper bar specimen is given in figure 7(h).

REFERENCES

1. Shaw, M. C., and Macks, E. F.: Analysis and Lubrication of Bearings. McGraw-Hill Book Co., Inc., 1949, p. 369.

2. Palsulich, J.: Tired Bearings - Reasons and Remedies. Lubrication Eng., vol. 8, no. 6, Dec. 1952, pp. 293-294, 313-314.

3. Bowden, F. P., and Tabor, D.: The Friction and Lubrication of Solids. The Clarendon Press (Oxford), 1950, p. 275.

4. Ackeret, J., and De Haller, P.: Ueber die Zerstörung von Werkstoffen durch Tropfenschlag und Kavitation. Schweizerische Bauzeitung, Bd. 108, Heft 10, Sept. 5, 1936, pp. 105-106.

5. Ackeret, J., and De Haller, P.: Ueber Werkstoffzerstörung durch Stosswellen in Flüssigkeiten. Schweizer Archiv angewandte Wiss. und Technik, Bd. 4, Nr. 10, Oct. 1938, pp. 293-294.

6. Brandenberger, E., and De Haller, P.: Untersuchungen über Tropfenschlagerosion. Schweizer Archiv angewandte Wiss. und Technik, Bd. 10, Nr. 11, Nov. 1944, pp. 331-341; Nr. 12, Dec. 1944, pp. 379-386.

7. Bondi, A.: Physical Chemistry of Lubricating Oils. Reinhold Pub. Corp., 1951, p. 16.

8. Nadai, A.: Theory of Flow and Fracture of Solids. Vol. I. Second ed., McGraw-Hill Book Co., Inc., 1950, p. 177.

9. Kolsky, H.: An Investigation of the Mechanical Properties of Materials at Very High Rates of Loading. Proc. Phys. Soc. (London), ser. B., vol. 62, no. 359, Nov. 1949, pp. 676-700.

10. Rizika, J. W., and Rohsenow, W. M.: Thermocouple Thermal Error. Ind. and Eng. Chem., vol. 44, no. 5, May 1952, pp. 1168-1171.

11. Dohrenwend, C. O., and Mehaffey, W. R.: Electrical Resistance Gauges and Circuit Theory. Handbook of Experimental Stress Analysis, John Wiley & Sons, Inc., 1950, pp. 177 ff.

TABLE 1

WEIGHT LOSS AND INCREMENT OF KNOOP HARDNESS AS FUNCTIONS OF TIME AND STATIC PRESSURE

Length of test, min	Static pressure, lb/sq in.	Weight loss, mg	Increment in Knoop hardness kg/sq mm
30	120	0.8	11
30	150	.5	6
30	200	.6	12
30	250	.3	4
60	120	1.6	22
60	150	1.4	22
60	200	.9	18
60	250	.4	14

TABLE 2

PEAK VALUE OF COMPRESSION WAVE TRANSMITTED ALONG SPECIMEN BAR AND PERMANENT STRAIN AT CONCLUSION OF EVERY TEST

[Duration of each test, 5 min]

Test	Peak value of transmitted compression wave, lb/sq in. gage	Compressive strain, μin./in., at distance from head end of specimen bar, in. -			
		5	6	7	8
1	2,000	90	90	78	70
2	2,000	100	90	80	74
3	2,400	100	90	80	74
4	2,400	100	90	80	74
5	4,600	160	135	118	98

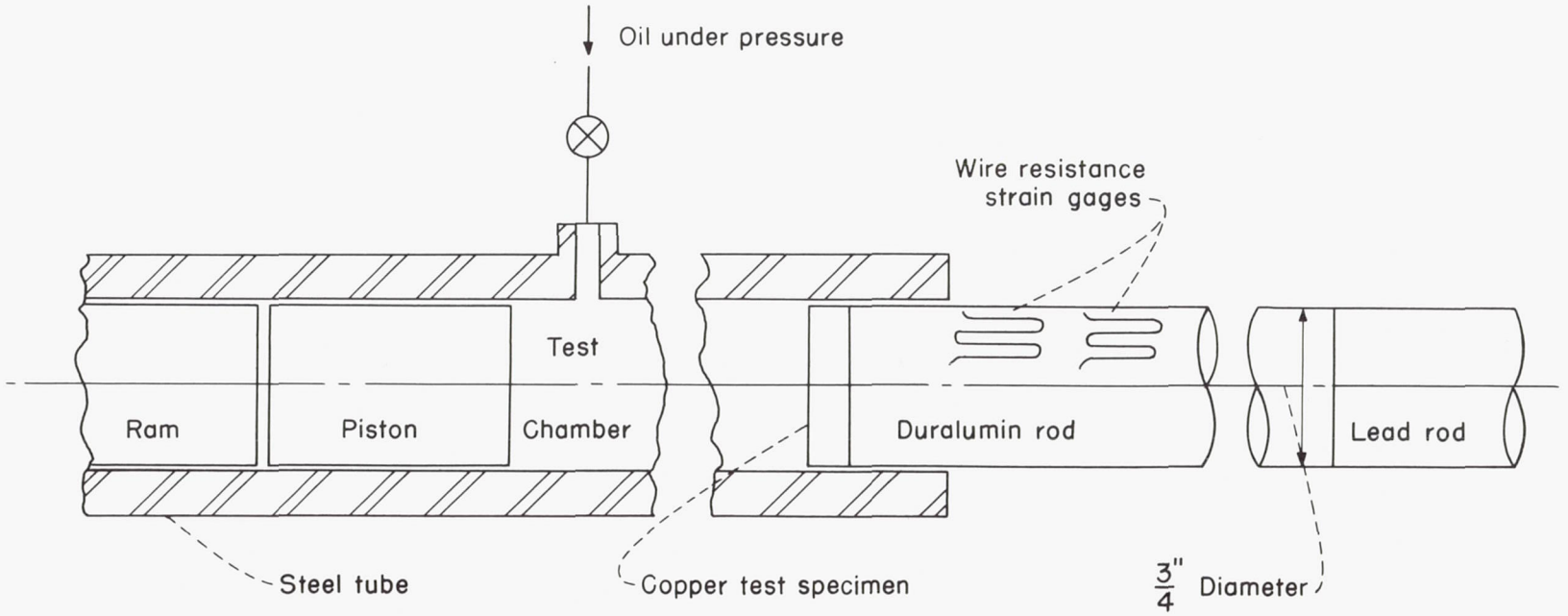

Figure 1.- Diagrammatic sketch of pressure-wave apparatus.

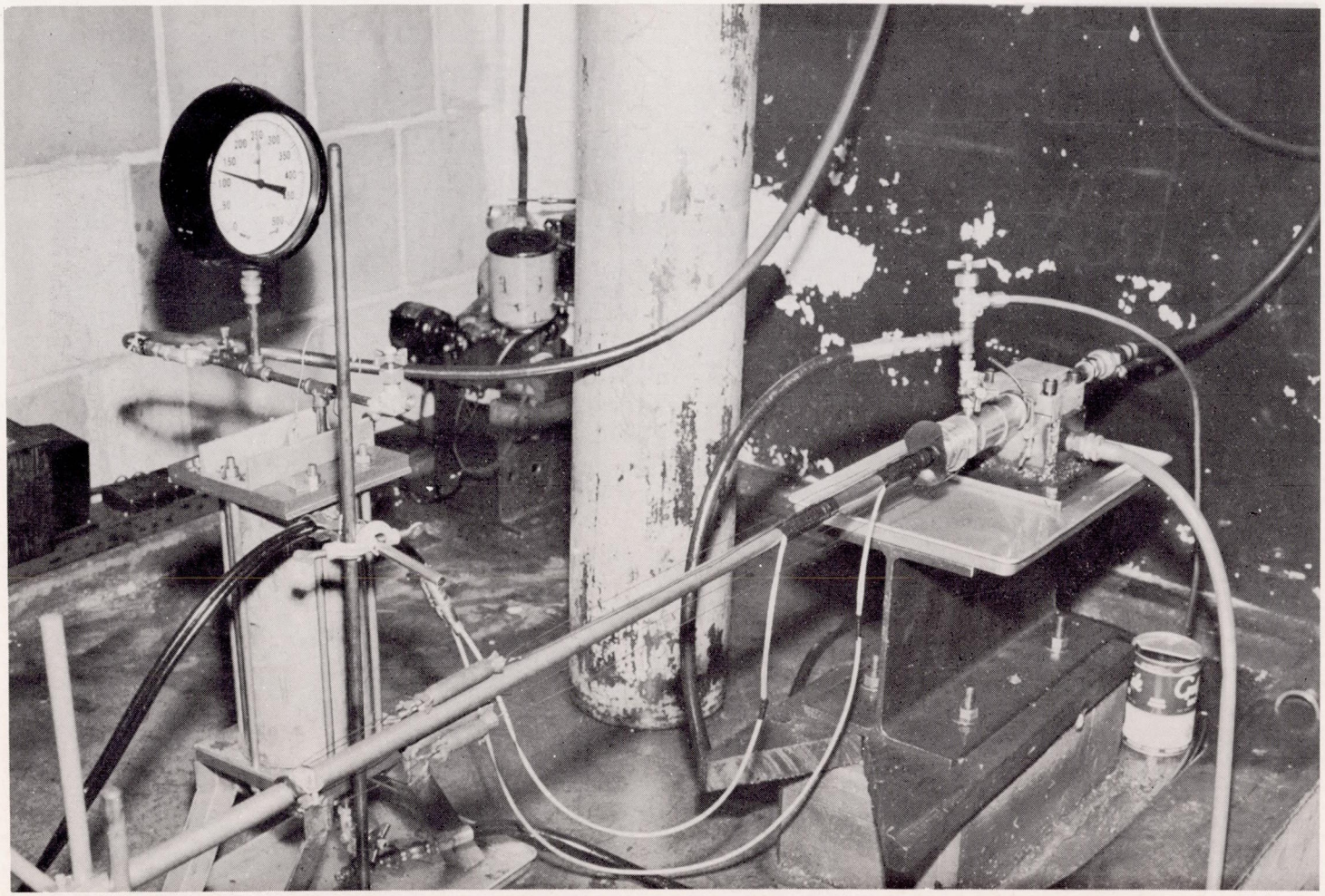

L-83604

Figure 2.- Photograph of pressure-wave apparatus showing air hammer at right, Duralumin gage rod, strain gages, nitrogen tank, oil tank, and pressure gage.

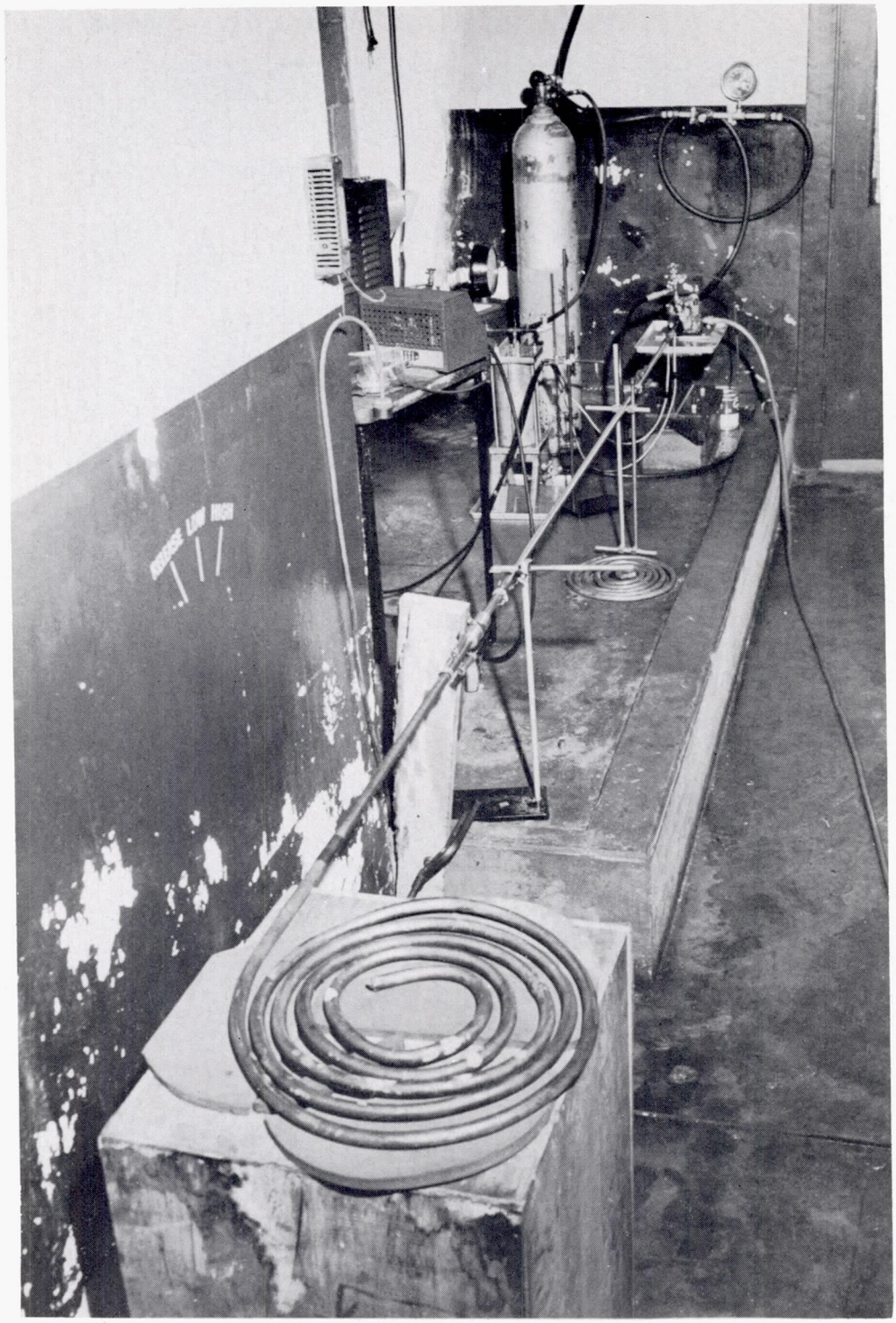

L-83605

Figure 3.- General view of pressure-wave apparatus showing air-pressure gage on far wall and coil of energy-absorbing lead rod in foreground.

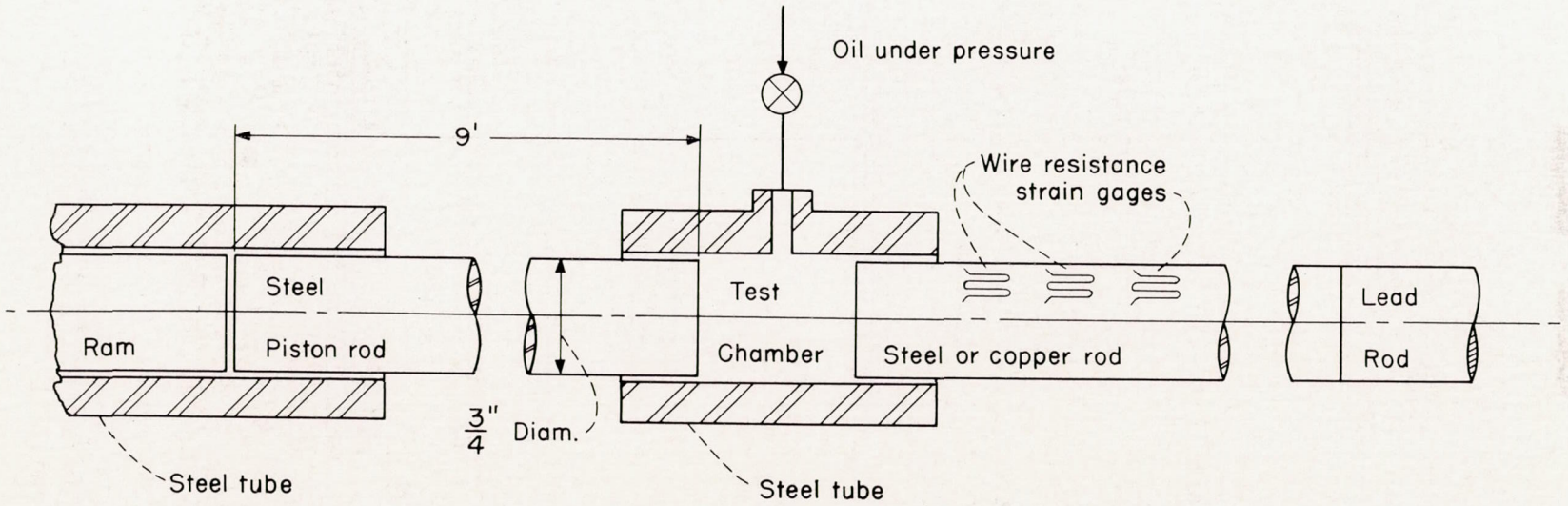

Figure 4.- Diagrammatic sketch of modified pressure-wave apparatus showing long piston rod.

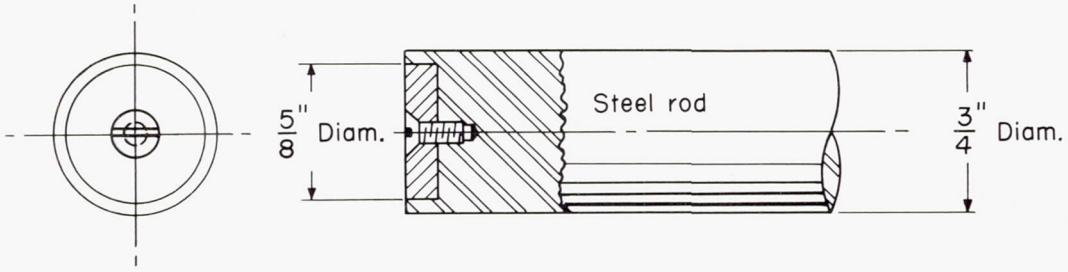

(a) Method of attaching specimen to Duralumin gage rod and initially to steel gage rod.

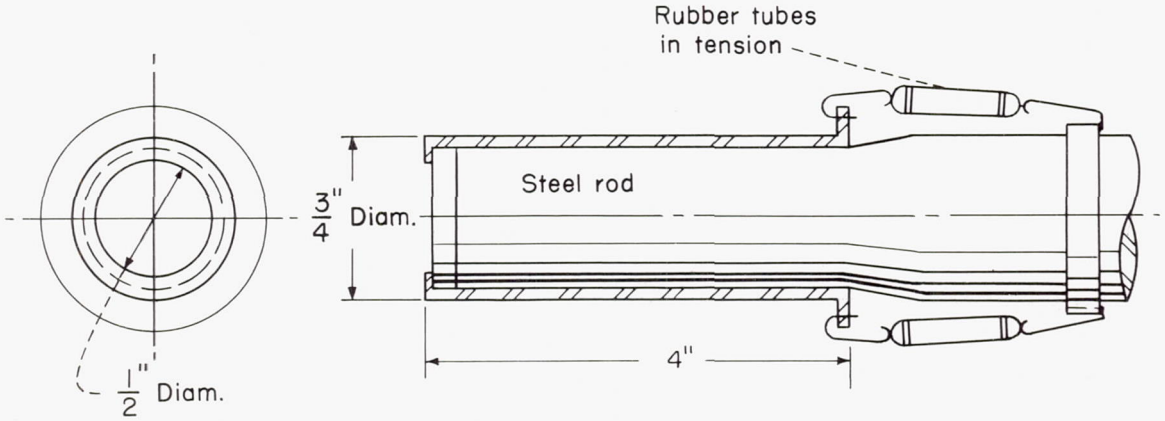

(b) Second method used for attaching specimen to steel gage rod.

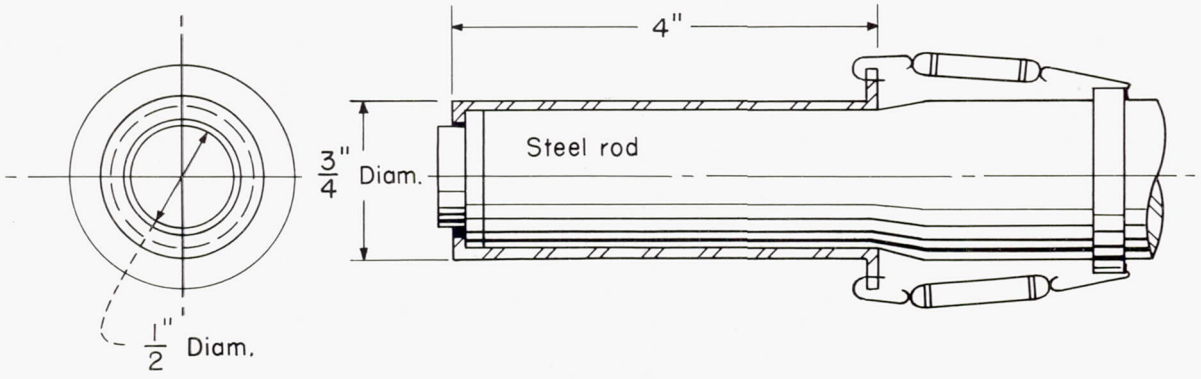

(c) Specimen shaped to experience hydrostatic stress.

Figure 5.- Specimens and methods of attachment used.

(a) Photomicrograph of specimen ready for testing.

(b) Photomicrograph of specimen after 60-minute test.

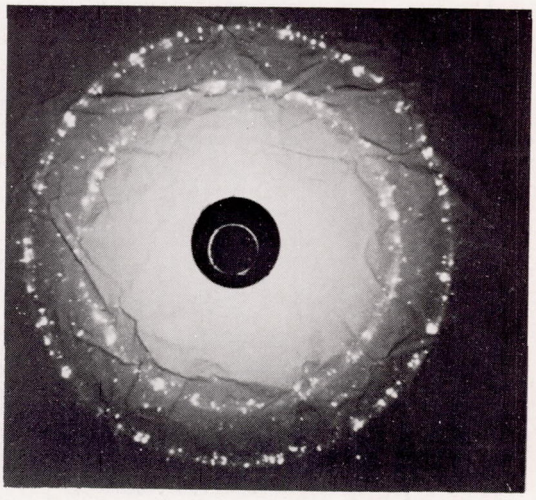

(c) X-ray diffraction picture of specimen ready for testing.

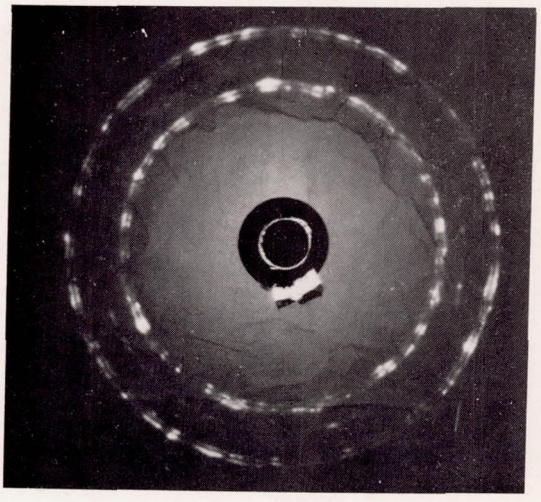

L-83606

(d) X-ray diffraction picture of specimen after 60-minute test.

Figure 6.- Photomicrographs and X-ray diffraction pictures of same annealed copper specimen showing results of cold-work.

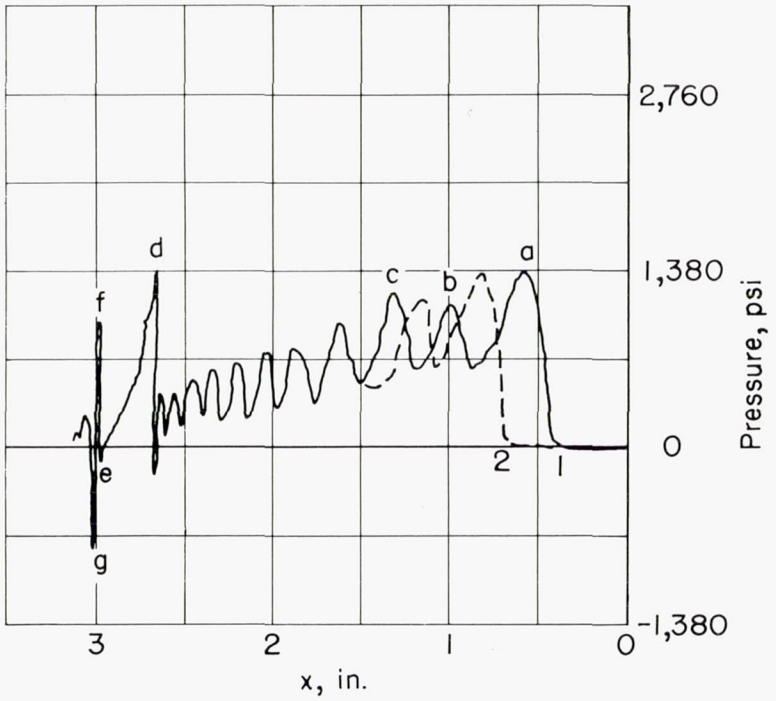

(a) Steel gage rod without specimen. Piston length, 3.25 inches; sweep direction, right to left; time constant of sweep, 190 microseconds; oil chamber, 9.75 inches; $(dp/dt)_1 \approx 120$ lb/sq in./μsec.

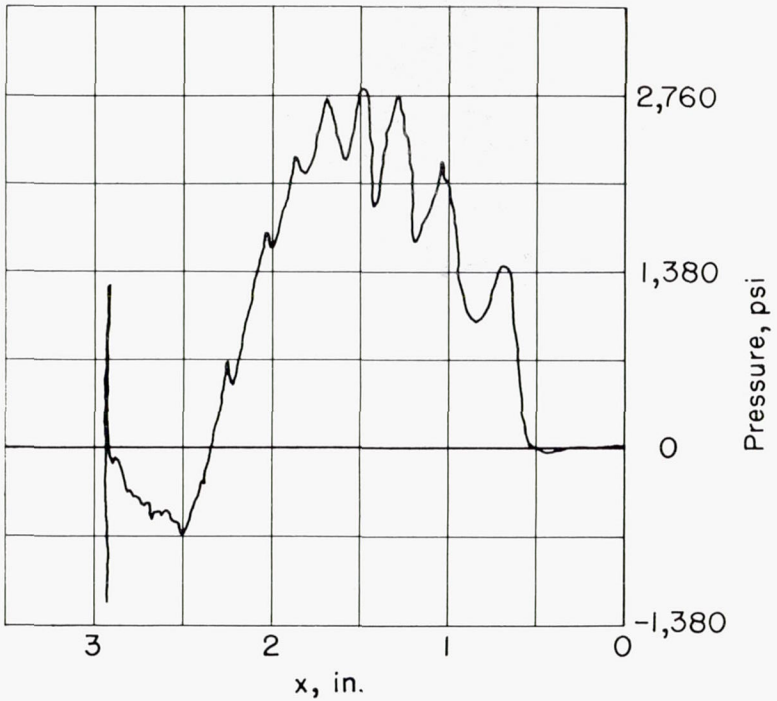

(b) Steel gage rod with specimen as in figure 5(b). Piston length, 3.25 inches; sweep direction, right to left; time constant of sweep, 160 microseconds; oil chamber, 0.844 inch.

Figure 7.- Oscillograms made at a static pressure of 300 lb/sq in. gage.

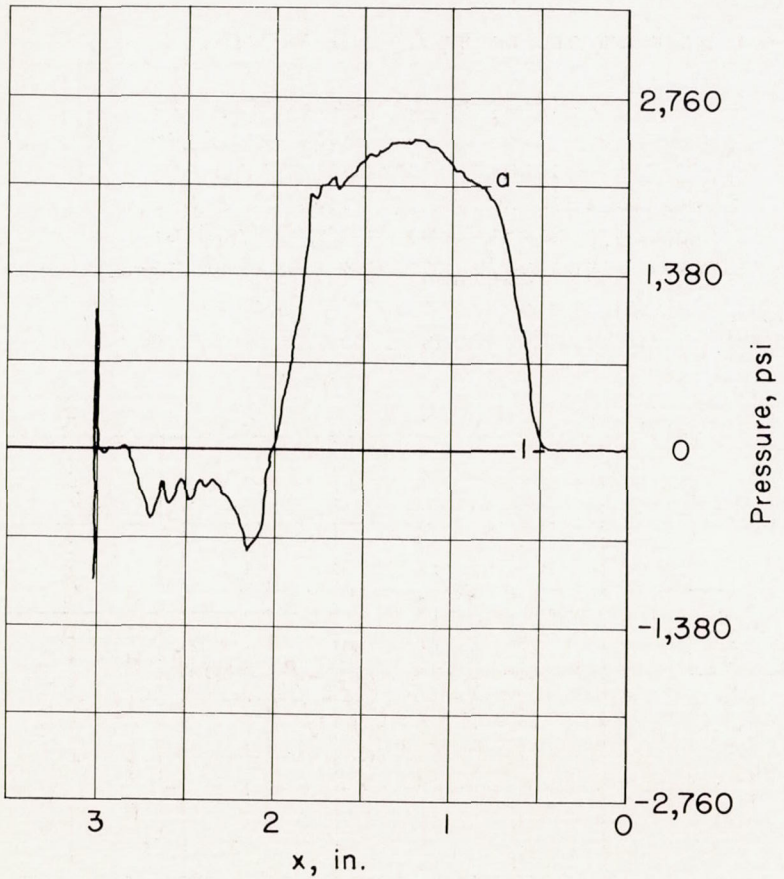

(c) Steel gage rod with specimen as in figure 5(b). Piston length, 3.25 inches; sweep direction, right to left; time constant of sweep, 160 microseconds; oil chamber, 0.312 inch; $(dp/dt)_1 \approx 105$ lb/sq in./μsec.

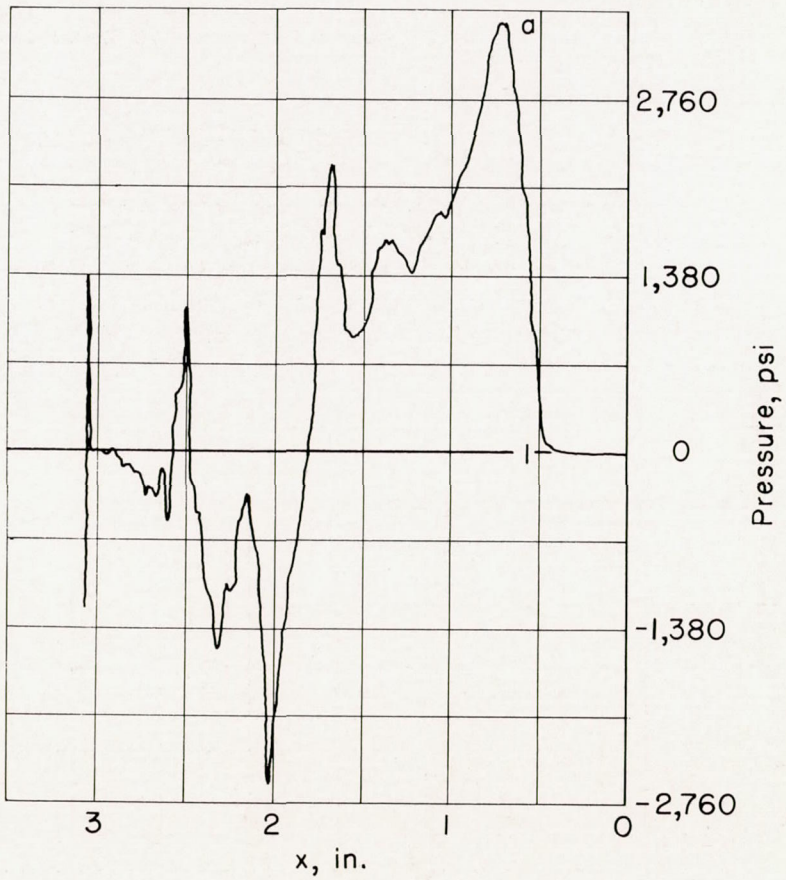

(d) Steel gage rod with specimen as in figure 5(b). Piston length, 3.25 inches; sweep direction, right to left; time constant of sweep, 160 microseconds; oil chamber, 0.094 inch; $(dp/dt)_1 \approx 270$ lb/sq in./μsec.

Figure 7.- Continued.

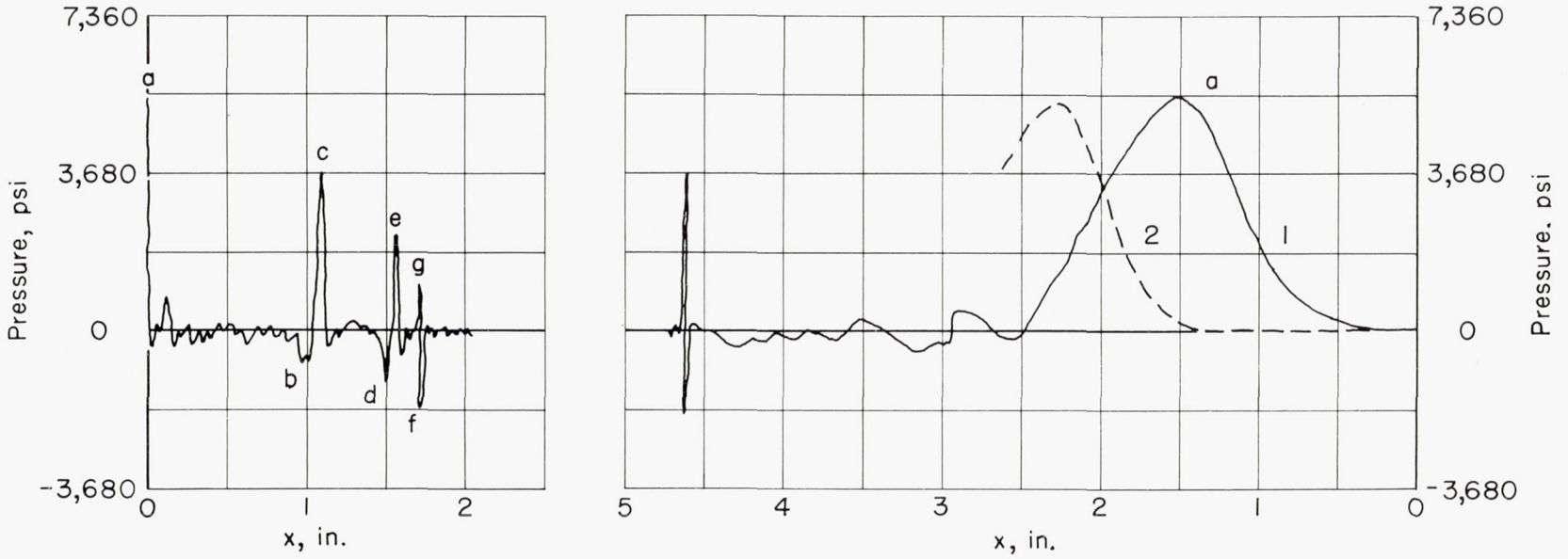

(e) Steel gage rod without specimen. Piston length, 9 feet; sweep direction, left to right; oil chamber, 0.062 inch.

(f) Steel gage rod without specimen. Piston length, 9 feet; sweep direction, right to left; time constant of sweep, 74 microseconds; oil chamber, 0.062 inch; $(dp/dt)_1 \approx 350$ lb/sq in./μsec.

Figure 7.- Continued.

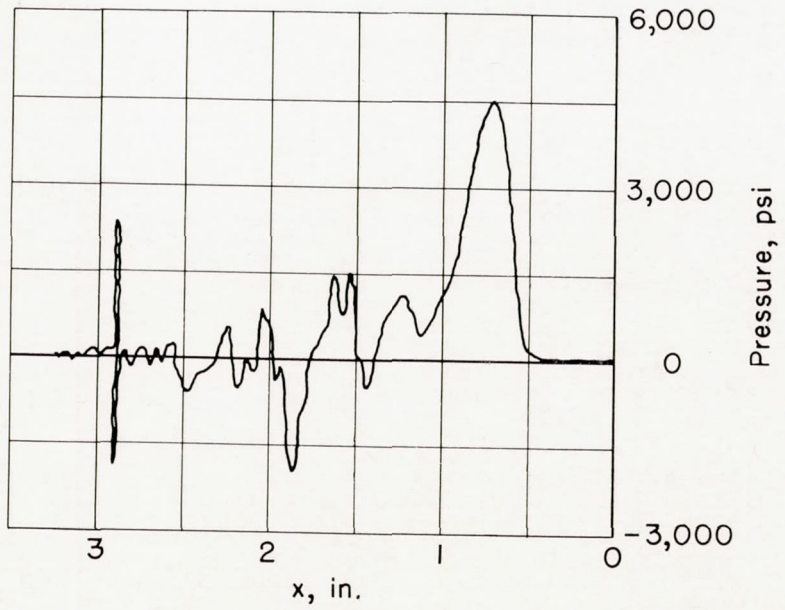

(g) Steel gage rod with specimen as in figure 5(b). Piston length, 9 feet; sweep direction, right to left; oil chamber, 0.094 inch.

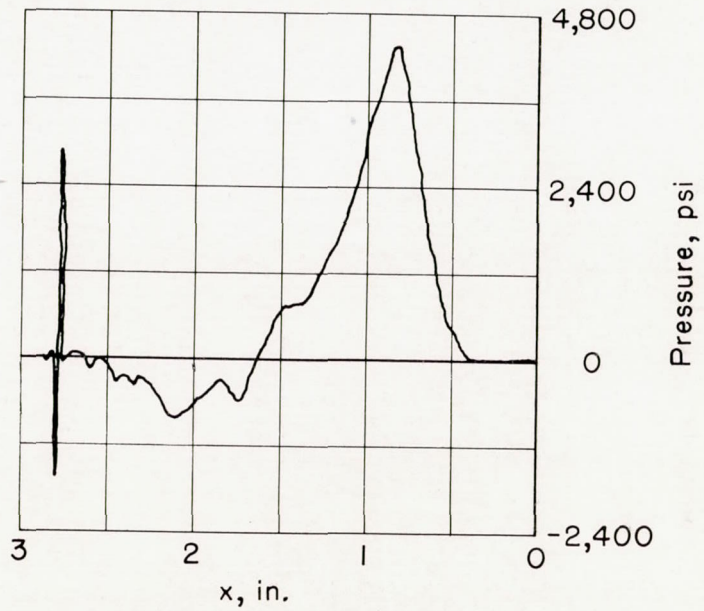

(h) Copper specimen rod. Piston length, 9 feet; sweep direction, right to left; oil chamber, 0.188 inch.

Figure 7.- Concluded.

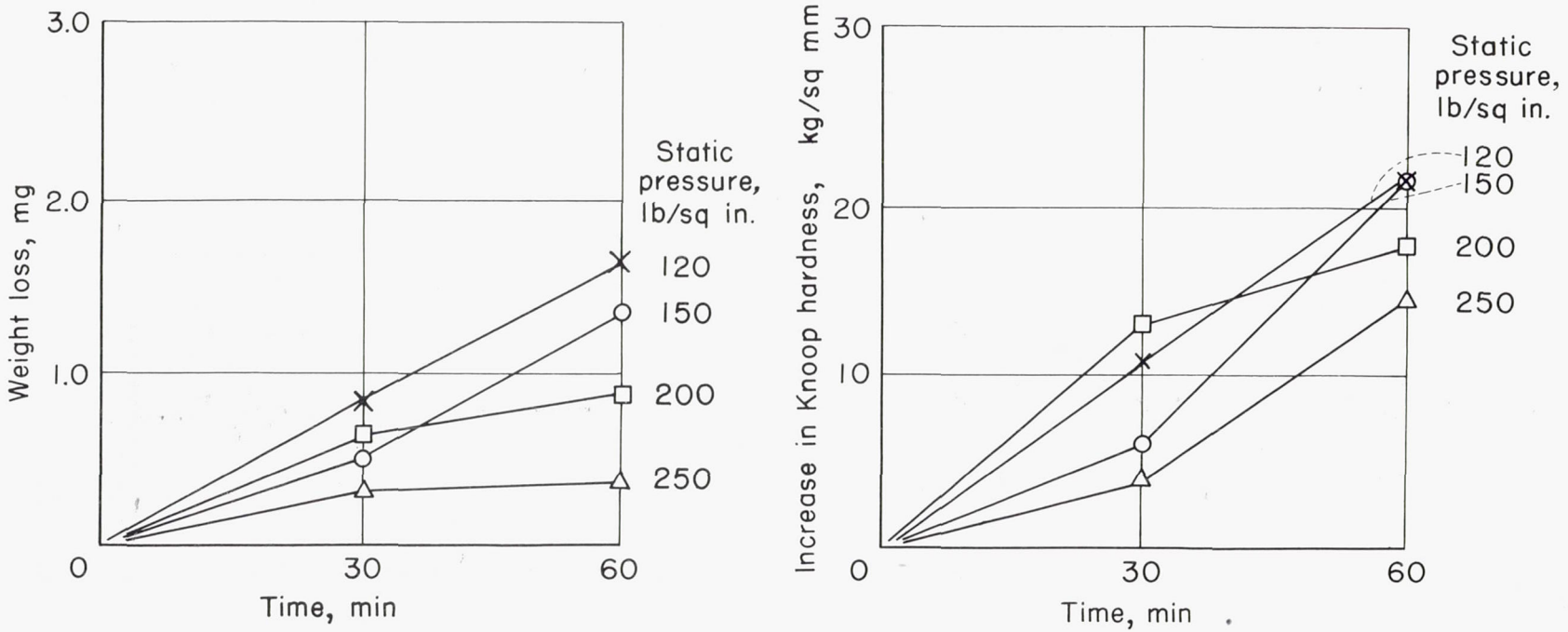

Figure 8.- Weight loss and increase in Knoop hardness as functions of time and static pressure.

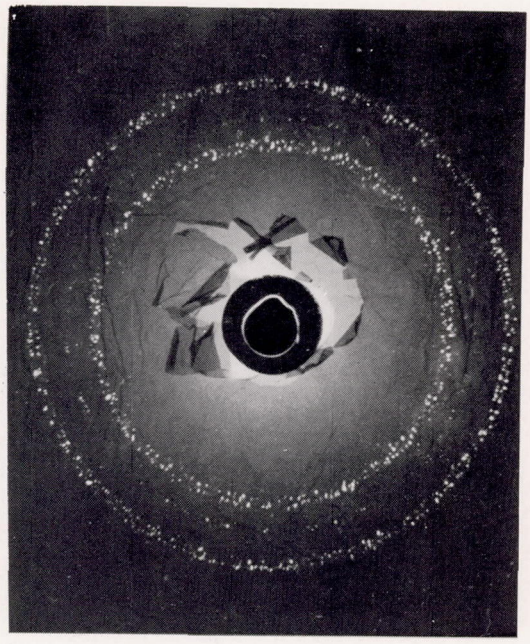

(a) Specimen ready for testing.

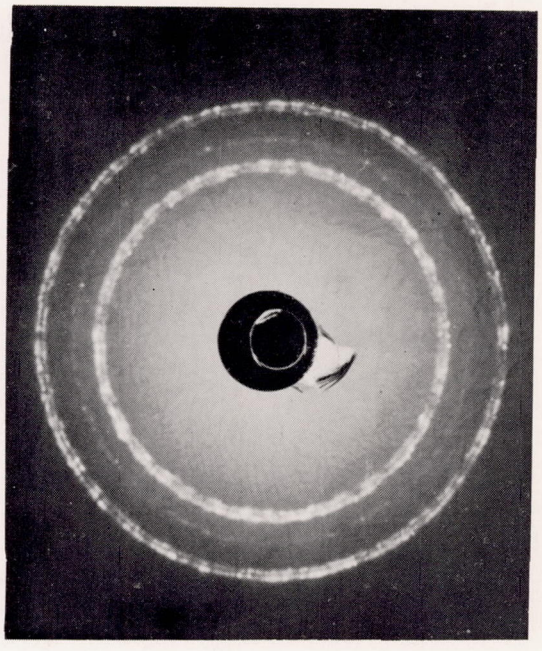

(b) Specimen after test of 15 minutes.

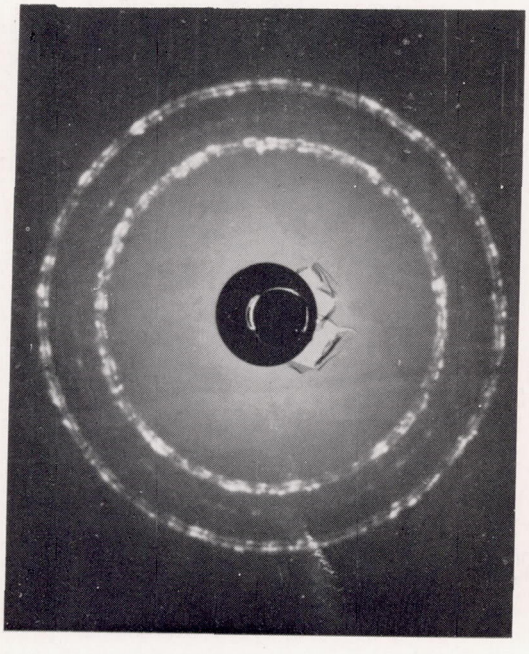

(c) Specimen etched to depth of 0.002 centimeter.

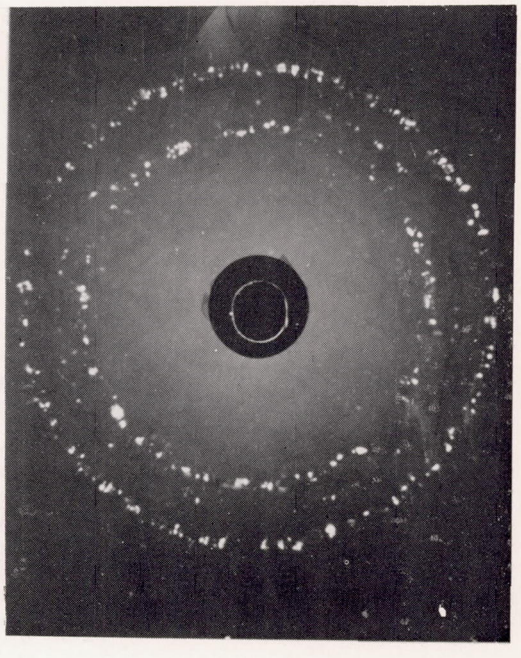

L-83607

(d) Specimen etched to depth of 0.006 centimeter.

Figure 9.- X-ray diffraction pictures of same annealed copper specimen in which successive layers were electrolytically etched away.

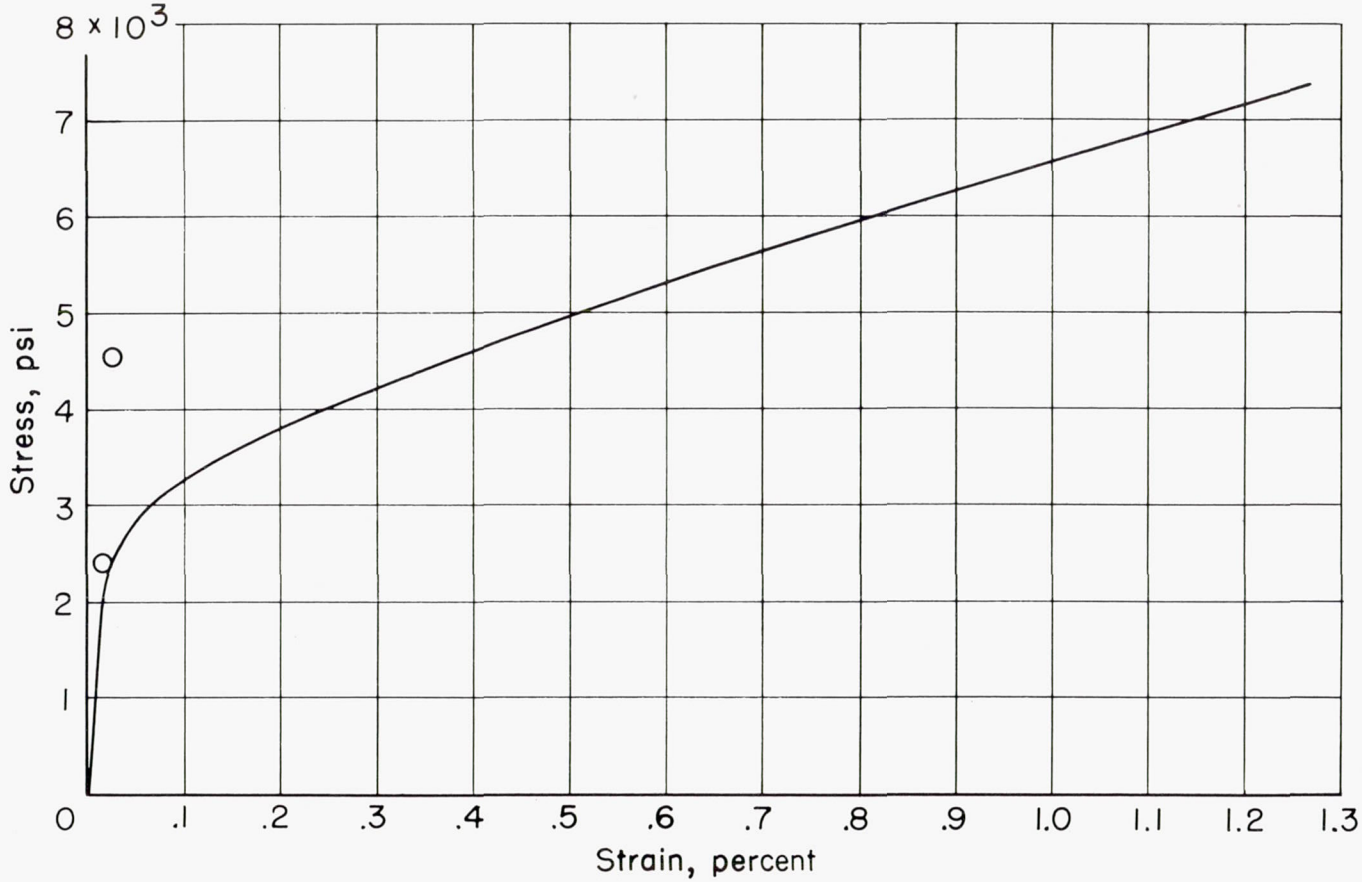

Figure 10.- Static tensile stress-strain curve of annealed commercial copper. Dynamic values are denoted by test-point symbols.

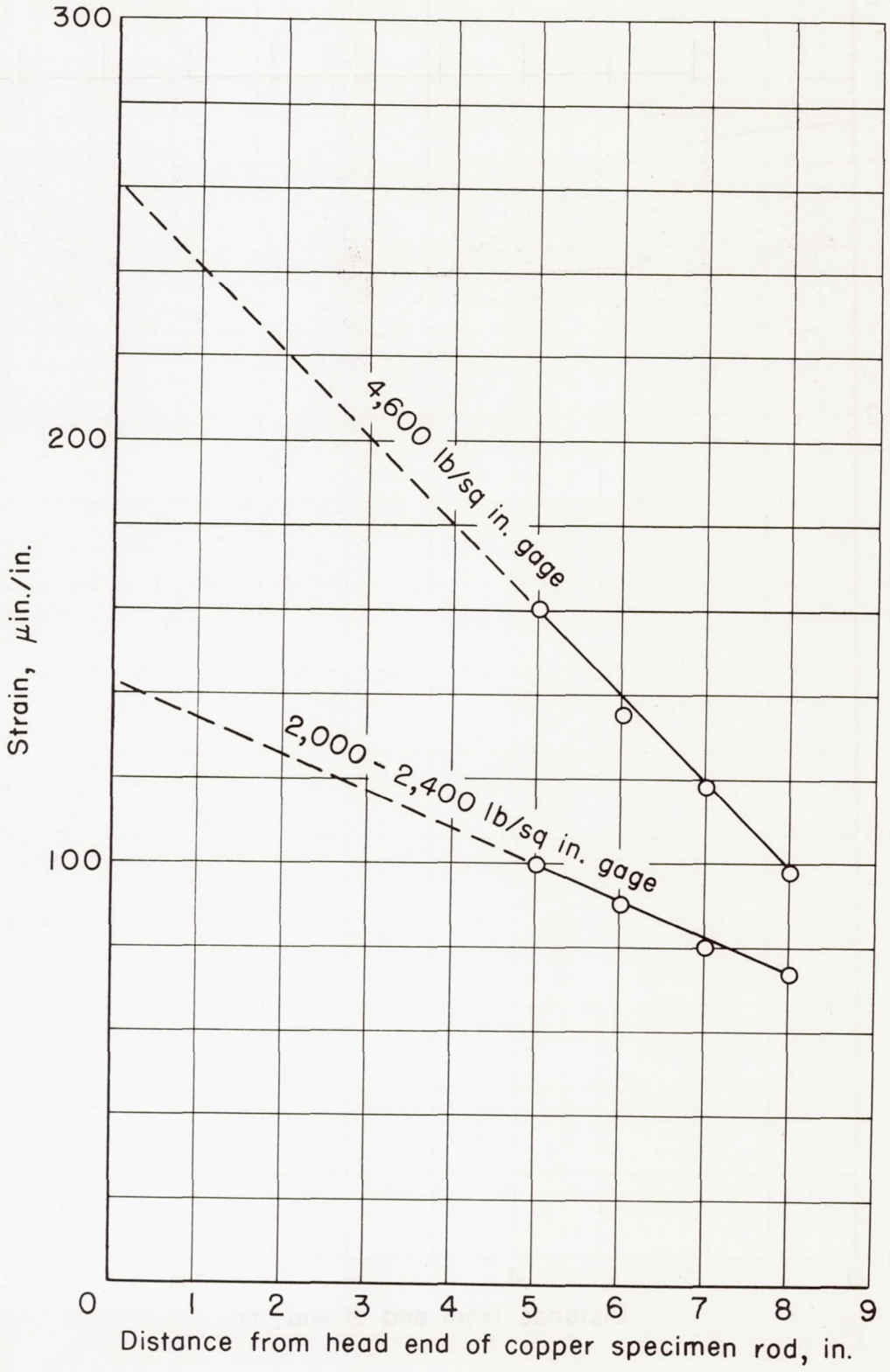

Figure 11.- Compressive strains against distance along specimen bar.

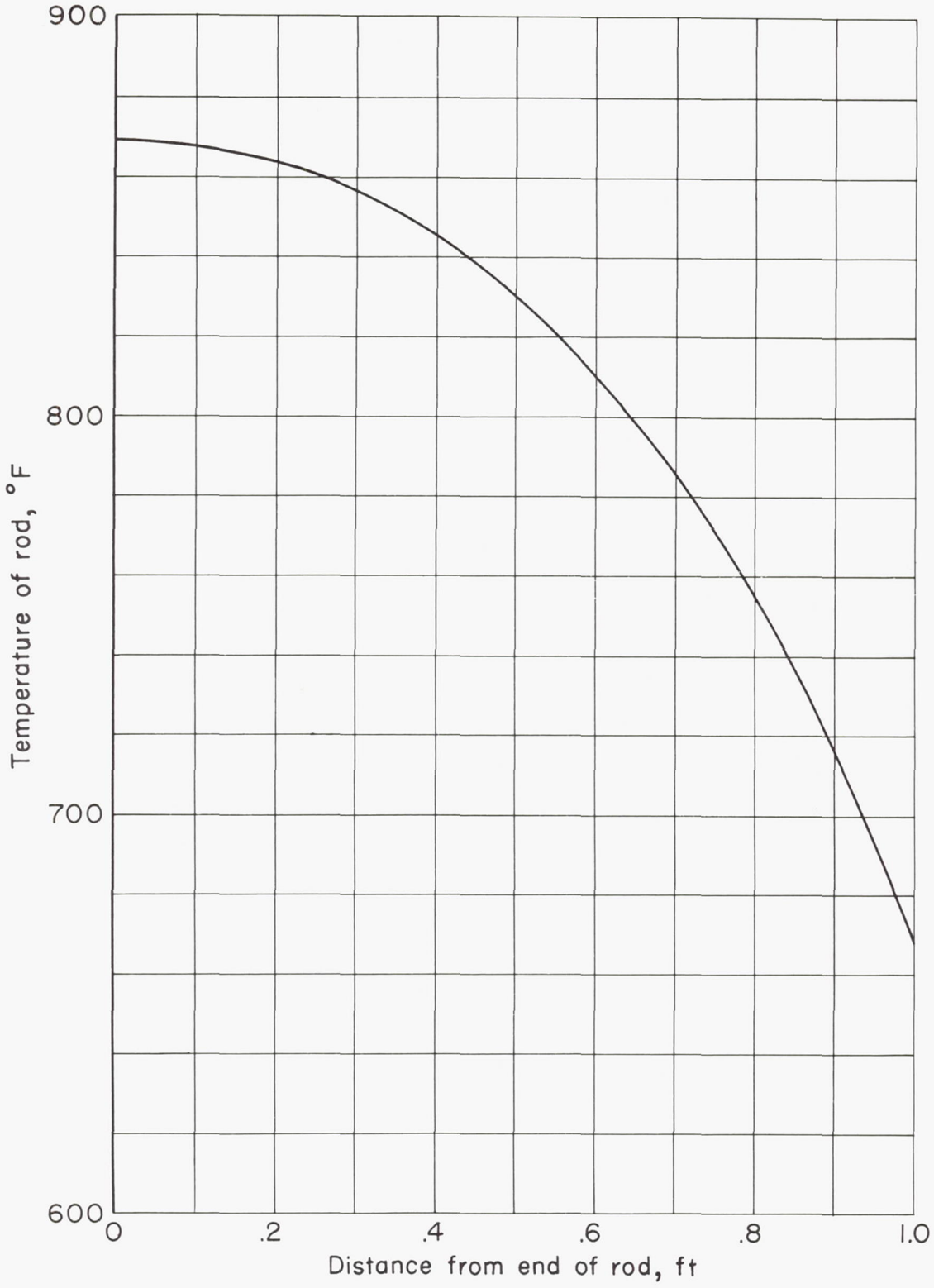

Figure 12.- Temperature distribution along copper bar in annealing furnace.

NACA-Langley - 6-22-54 - 1000